LASER SYSTEM COMPONENTS

Formation of two-dimensional monochromatic images of a laser jet by a spherically bent mica crystal

Quantum Electronics **24** (4) 356–358 (1994)

LASER SYSTEM COMPONENTS

PACS numbers: 52.70.La; 52.25.Nr

Formation of two-dimensional monochromatic images of a laser jet by a spherically bent mica crystal

B A Bryunetkin, V M Dyakin, S A Pikuz, T A Pikuz, A Ya Faenov

Abstract. Two-dimensional x-ray images were obtained for a laser-generated plasma jet as it collided with an obstacle and expanded in a static magnetic field. A mica crystal bent to form a spherical surface of 100 mm radius was used. The images were formed by the radiation representing the resonance and inter-combination lines of the Mg XI ion. A shock-compressed zone formed near the obstacle and the expansion cone of the Mg XI ions became narrower in a transverse magnetic field. The spatial resolution in the plane of the image was better than 100 μm for objects of large linear dimensions (~10 mm).

The methods of imaging spectroscopy [1] can provide valuable information on the structure and dynamics of plasma objects. These methods are particularly effective in studies of the influence of external agencies or events on a plasma, for example, a collision of a laser plasma with an obstacle [2], the expansion of a laser plasma in the presence of a background gas [3] or external magnetic field [4], or the interaction of laser plasma fluxes [5].

In the x-ray range it is possible to form two-dimensional images with the aid of crystals bent to form a spherical surface [6]. The spatial resolution along one of the directions (usually in the direction of expansion of a laser plasma jet) is provided by the focusing properties of the spherical surface (sagittal plane), whereas the dispersive properties of such a bent crystal are employed in the perpendicular direction (meridional plane).

We shall now consider the ray paths in the meridional plane, shown in Fig. 1, where a is the distance from the object to the vertex of the bent crystal, b is the distance from the vertex of the crystal to the image, H is the size of the crystal in the meridional plane, and R is the radius to which the crystal is bent. The glancing angle θ of the radiation at the crystal vertex is related to the wavelength by the Bragg condition:

$$2d_n \sin\theta = n\lambda, \tag{1}$$

where n is the reflection order; $2d_n$ is twice the interplanar distance for the n-th reflection order. The distances a and b are related by the focusing condition in the sagittal plane:

$$\frac{1}{a}+\frac{1}{b}=\frac{1}{f_s}, \tag{2}$$

B A Bryunetkin, V M Dyakin, A Ya Faenov Scientific-Production Centre, 'VNIIFTRI', Mendeleevo, Moscow Province
S A Pikuz P N Lebedev Physics Institute, Russian Academy of Sciences, Moscow
T A Pikuz State Technical University, Moscow

Received 24 August 1993
Kvantovaya Elektronika **21** (4) 382–384 (1994)
Translated by A Tybulewicz

where $f_s = R/2\sin\theta$ is the sagittal focal length. Subject to Eqn (2), the magnification in the sagittal plane is

$$\sigma = b/a = R/(2a\sin\theta - R), \tag{3}$$

and in the meridional plane it is

$$v = g/c = \left|\frac{R[a - \sin\theta(2a\sin\theta - R)]}{(R\sin\theta - a)(2a\sin\theta - R)}\right|. \tag{4}$$

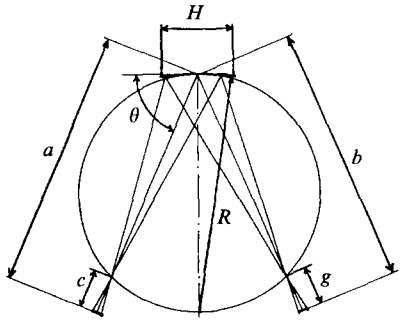

Figure 1. Ray paths in the meridional plane of a spherically bent crystal.

It is evident from Eqns (3) and (4) that the same magnifications can be obtained for $\theta = \pi/2$ and they can be arbitrary [6]. The normal incidence is typical of x-ray microscopes, usually operating under high magnification conditions (see, for example, Refs 7 and 8). However, normal-incidence systems have a significant shortcoming: an image can be constructed only at wavelengths close to multiple fractions of the doubled interplanar distance ($\lambda = 2d_n/n$), i.e. the set of wavelengths limited by the available crystals.

From the practical point of view it is highly desirable to be able to form two-dimensional images of plasma objects of large dimensions (of the order of several millimetres) at an arbitrary wavelength of the source radiation. Such a variant of the use of a spherical crystal is demonstrated below. An analysis of Eqns (3) and (4) shows that there is a certain range of distances from the object to the crystal vertex such that the magnifications are of comparable magnitude: $\sigma/v = 0.3-3$; the images can then be obtained at any wavelength in the range $(1/\sqrt{2})2d_n/n < \lambda < 2d_n/n$. In particular, if the distance from the object to the crystal vertex is twice the sagittal focal length ($a = R/\sin\theta$), the magnifications are the same and equal to unity: $\sigma = v = 1$.

We used a mica crystal of 30 mm × 10 mm dimensions bent to form a sphere of radius $R = 100$ mm and operating in the second reflection order ($n = 2$, $d_2 = 993.893$ pm). Plasma was generated by Nd glass laser radiation of energy

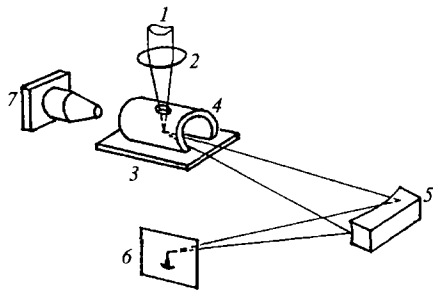

Figure 2. Apparatus used in a study of the interaction of a laser plasma with a tubular obstacle: (*1*) laser radiation; (*2*) focusing objective; (*3*) Mg target; (*4*) tubular obstacle; (*5*) crystal; (*6*) photographic film; (*7*) pinhole camera.

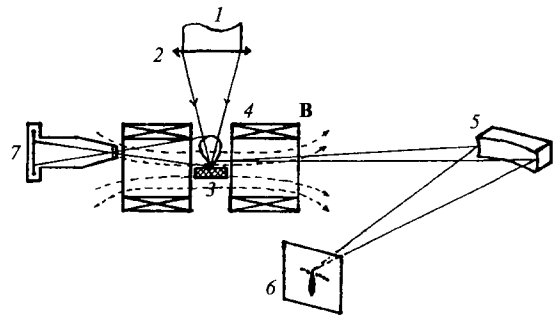

Figure 4. Apparatus used in observation of the expansion of a plasma in a static magnetic field: (*1*) laser radiation; (*2*) focusing objective; (*3*) Mg target; (*4*) solenoid; (*5*) crystal; (*6*) photographic film; (*7*) pinhole camera.

up to 30 J in the form of pulses of 2 ns duration at half-amplitude. This radiation was focused in vacuum onto the surface of a bulk flat magnesium target. The images of a plasma jet formed in this way were recorded by using the radiation representing the resonance (R) and intercombination (I) lines of the He-like Mg XI ion (λ_R = 0.9169 nm, λ_I = 0.9231 nm). Photographs were recorded on Kodak DEF-2 film protected from the visible and infrared radiation by a Be filter, which was 6.5 μm thick. On the side diametrically opposite the crystal there was an x-ray pinhole camera with an aperture 150 μm in diameter closed by a Mylar filter coated on both sides by Al films whose total thickness was 0.3 μm (E_{cutoff} = 0.3 keV).

In the first series of experiments an obstacle in the shape of a cylinder cut along a generator was placed in the path of the expanding plasma (Fig. 2). Pinhole images and two-dimensional monochromatic images were obtained with the R and I lines of the Mg XI ion (Fig. 3, magnification $\sigma = \nu = 1$). A characteristic shock-wave structure was observed which appeared when of the plasma interacted with the obstacle [9]. The width of the radiation-emitting zone could be estimated from the following expression [9]:

$$\Delta z \simeq 3 \times 10^{-11} Z^{-1} N_e^{-1} u^4, \qquad (5)$$

where u and Z are the velocity and the average charge of the incident ions; N_e is the electron density in the unperturbed plasma near the obstacle. Estimates based on our earlier measurements (Z = 10, $N_e = 3 \times 10^{17}$ cm^{-3}; $u = 3 \times 10^7$ cm s^{-1}) yielded $\Delta z \approx 0.8$ mm for the width of the radiation-emitting zone, which is in agreement with the results presented in Fig. 3.

The plasma expansion in a magnetic field was observed in the configuration shown schematically in Fig. 4. A magnetic field up to 3 T was generated by a two-section solenoid and was directed parallel to the target surface. Observations were made along the solenoid axis. The pinhole and monochromatic images (obtained with the magnifications σ = 1/3 and ν = 1/6, respectively) clearly demonstrated (Fig. 5) the formation of a plasma jet in a transverse magnetic field. Similar effects had been observed earlier by us [10] and also by other authors [11, 13]. They were tentatively attributed to the development of flute instabilities. A detailed analysis of this effect is outside the scope of the present study, but it should be pointed out that the plasma observed in the cited investigations consisted primarily of ions with a low charge (Z = 2–4) and was of relatively low density ($N_e \approx 10^{15}$–10^{16} cm^{-3}), so that the formation of a jet of ions with a high

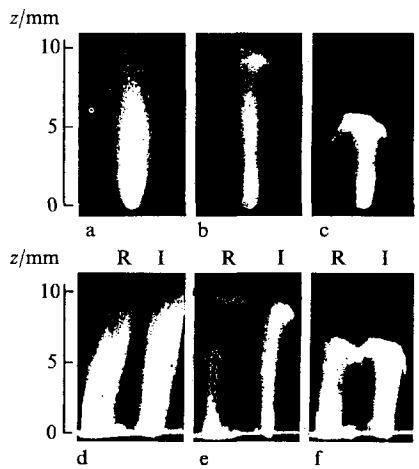

Figure 3. Pinhole images (a–c) and the images obtained with the aid of the R and I lines (d–f) of a laser plasma interacting with a tubular obstacle of radius r = 10 mm (b, e) and 6 mm (c, f), as well as under free-expansion conditions (a, d).

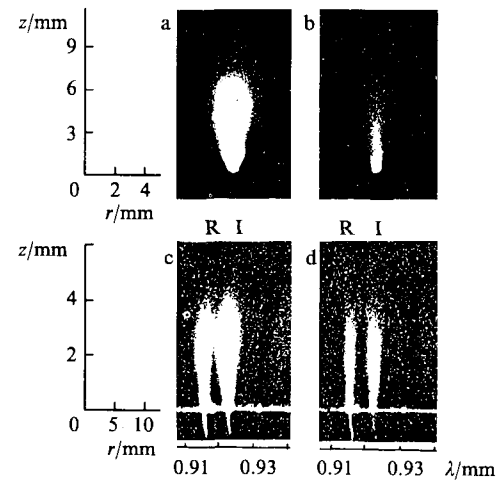

Figure 5. Pinhole images (a, b) and the images obtained with the aid of the R and I lines of the Mg XI ions (c, d) of a laser plasma jet in the absence (a, c; B = 0) and in the presence (b, d; B = 3 T) of a static magnetic field.

charge ($Z \approx 10-12$) in a transverse magnetic field was observed by us for the first time.

In the concluding stage of our investigation we estimated the spatial resolution. The resolution in the meridional and sagittal planes was subject to the influence of different physical factors. In the sagittal plane the spatial resolution was governed by the aberrations of the spherical surface of the crystal and under our experimental conditions it amounted to ~ 20 μm. In the meridional plane the resolution was influenced by the size of the source and its nonmonochromaticity. The resolution governed by these factors can be described by the following expressions which apply to the sagittal and meridional planes, respectively:

$$\delta r_s = \left[d^2 R^2 / 8R(a - R\sin\theta)^2\right] \cot\theta, \quad (6)$$

$$\delta r_\lambda = \delta\lambda / D_r = (d\lambda/\lambda) R \tan\theta, \quad (7)$$

where d is the size of the source; $\delta\lambda$ is the width of the spectral line; $D_r = (\lambda/R)\cot\theta$ is the dispersion. The influence of these factors is different in different parts of the laser jet: near the target the main role is played by the source nonmonochromaticity, whereas during the subsequent stages of the expansion the main factor is the source size.

The apparatus used to determine the spatial resolution was similar to the configurations shown in Figs. 2 and 4, except that instead of the image of a plasma jet we focused onto the film the image of a test object located at a distance of ~ 1 cm from the plasma, i.e. the plasma was used to provide the background illumination of the test object. The object was in the form of two superimposed metal grids, one with a period of 3.1 mm and formed by wires 0.5 mm thick, and the other with a period of 0.46 mm and formed by wires 0.1 mm thick.

The results obtained (Fig. 6) showed that in the sagittal plane the resolution was better: it was ~ 100 μm (the thinner wires were resolved). In the meridional plane the situation was more complex: the 0.1 mm (100 μm) thick wires were resolved only at large distances from the target. Estimates based on Eqns (6) and (7) indicated that this was associated with the large width of the observed lines near the target when the heating radiation had the following parameters: $\delta\lambda/\lambda \approx 3\times10^{-3}$ for the R and I lines, so that $\delta r_\lambda \approx 0.5$ mm $\gg \delta r_s$. During the subsequent stages of the expansion the approximate equality $\delta r_\lambda \approx \delta r_s \approx 100$ μm was confirmed experimentally.

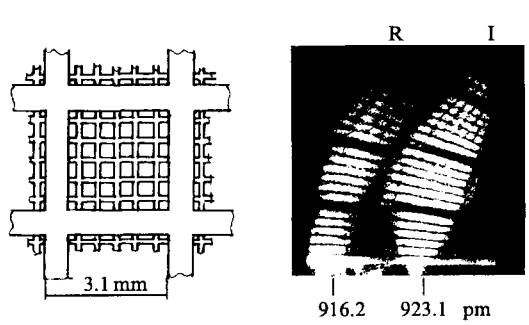

Figure 6. Test object and the results of the determination of the spatial resolution obtained with the aid of the R ($1s^2\,{}^1S_0 - 1s2p\,{}^1P_1$) and I ($1s^2\,{}^1S_0 - 1s2p^3P_1$) lines of the Mg XI ions.

Our study demonstrated that two-dimensional monochromatic x-ray images of large (in excess of 10 mm) plasma objects can be formed by a spherically bent mica crystal for arbitrary angles of incidence of the radiation. The strong reflection by a mica crystal in the I–V, VII, VIII, and XI orders makes it possible to cover practically the whole spectral range from 0.15 to 1.9 nm. Use of such a crystal provides extensive opportunities for the investigation of the structure and dynamics of plasma objects by x-ray imaging spectroscopy.

References

1. Bryunetkin B A, Pikuz S A , Skobelev I Yu, Faenov A Ya. *Laser Part. Beams* **10** 849 (1992)
2. Boĭko V A, Bryunetkin B A, Bunkin F V, et al. *Fiz. Plazmy* **10** 999 (1984) [*Sov. J. Plasma Phys.* **10** 573 (1984)]
3. Begimkulov U Sh, Bryunetkin B A, Dyakin V M, et al. *J. Phys. D* **25** 1583 (1992)
4. Begimkulov U Sh, Bryunetkin B A, Dyakin V M, et al. *Laser Part. Beams* **10** 723 (1992)
5. Begimkulov U Sh, Bryunetkin B A, Dyakin V M, et al. *Kvantovaya Elektron. (Moscow)* **18** 877 (1991) [*Sov. J. Quantum Electron.* **21** 794 (1991)]
6. Boiko V A, Vinogradov A V, Pikuz S A, Skobelev I Yu, Faenov A Ya *J. Sov. Laser Res.* **6** 85 (1985)
7. Williams M L, et al., Preprint No. 1, Lebedev Physics Institute, Academy of Sciences of the USSR, Moscow, 1990
8. Forster E, Gabel K, Uschmann I *Laser Part. Beams* **9** 135 (1991)
9. Boiko V A, Bryunetkin B A, Bunkin F V, et al. *Plasma Phys. Controlled Fusion* **26** 971 (1984)
10. Bryunetkin B A, Begimkulov U Sh, Dyakin V M, et al. *Kvantovaya Elektron. (Moscow)* **19** 246 (1992) [*Sov. J. Quantum Electron.* **22** 223 (1992)]
11. Mostovych A N, Ripin B H, Stamper J A *Phys. Rev. Lett.* **62** 2837 (1989)
12. Ripin B H, Manka C K, Peyser T A, et al. *Laser Part. Beams* **8** 183 (1990)